

1 *The present paper submitted to EarthArXiv is a non-peer reviewed preprint. The preprint was submitted to a*
2 *CATENA journal for peer review.*

3 *Climatic data: [https://protezionecivile.puglia.it/centro-funzionale-decentrato/rete-di-monitoraggio/annali-e-](https://protezionecivile.puglia.it/centro-funzionale-decentrato/rete-di-monitoraggio/annali-e-dati-idrologici-elaborati/annali-idrologici-parte-i-dati-storici/)*
4 *dati-idrologici-elaborati/annali-idrologici-parte-i-dati-storici/*

5 *Streamflow data: [https://protezionecivile.puglia.it/centro-funzionale-decentrato/rete-di-monitoraggio/annali-e-](https://protezionecivile.puglia.it/centro-funzionale-decentrato/rete-di-monitoraggio/annali-e-dati-idrologici-elaborati/annali-idrologici-parte-ii-download/)*
6 *dati-idrologici-elaborati/annali-idrologici-parte-ii-download/*

7 *Monthly sediment load are derived from the paper: <https://doi.org/10.1016/j.catena.2018.02.015>*

8

9 **MODELLING FOREST FIRE AND POST-FIRE MANAGEMENT IN A CATCHMENT**
10 **PRONE TO EROSION: Impacts on sediment yield**

11 De Girolamo Anna Maria^{(a)*}, Cerdan Olivier^(b), Grangeon Thomas^(b), Ricci Giovanni Francesco^(c),
12 Vandromme Rosalie^(b), Lo Porto Antonio^(a)

13 * Corresponding author: annamaria.degirolamo@ba.irsra.cnr.it

14

15 De Girolamo Anna Maria; Water Research Institute, National Research Council, Bari, Italy, annamaria.degirolamo@ba.irsra.cnr.it

16 Cerdan Olivier; Bureau de Recherches Géologiques et Minières, Département Risques et Prévention, Orléans, France, o.cerdan@brgm.fr

17 Grangeon Thomas, Bureau de Recherches Géologiques et Minières, Département Risques et Prévention, Orléans, France, t.grangeon@brgm.fr

18 Ricci Giovanni Francesco^(c); University of Bari Aldo Moro, Department of Agricultural and Environmental Sciences, Bari, Italy,
19 giovanni.ricci@uniba.it

20 Vandromme Rosalie^(b); Bureau de Recherches Géologiques et Minières, Département Risques et Prévention, Orléans, France, r.vandromme@brgm.fr

21 Lo Porto Antonio^(a); Water Research Institute, National Research Council, Bari, Italy, antonio.loporto@ba.irsra.cnr.it

22

23

24

25 **MODELLING FOREST FIRE AND POST-FIRE MANAGEMENT IN A CATCHMENT**
26 **PRONE TO EROSION: Impacts on sediment yield**

27 De Girolamo Anna Maria^{(a)*}, Cerdan Olivier^(b), Grangeon Thomas^(b), Ricci Giovanni Francesco^(c),
28 Vandromme Rosalie^(b), Lo Porto Antonio^(a)

29 (a) Water Research Institute, National Research Council, Bari, Italy

30 (b) Bureau de Recherches Géologiques et Minières, Département Risques et Prévention, Orléans, France

31 (c) University of Bari Aldo Moro, Department of Agricultural and Environmental Sciences, Bari, Italy

32 * Corresponding author: annamaria.degirolamo@ba.irsra.cnr.it

33 **Abstract**

34 *Forest fires change soil surface properties, alter the hydrological processes, and increase soil erosion. Post-*
35 *fire rehabilitation measures are useful to mitigate the effect of fire on soil erosion. This work aims to predict*
36 *the effects of forest fires and post-fire mitigation measures on runoff and specific sediment yield (SSY) in a*
37 *river basin (Celone, S-E Italy). The Soil and Water Assessment Tool model, calibrated with field*
38 *observations, was used to evaluate runoff and SSY for the current land use (baseline) and six post-fire*
39 *scenarios. From 1990 to 2011, at the basin scale, the average annual SSY was $5.60 \text{ t ha}^{-1} \text{ y}^{-1}$ ($SD = 3.47 \text{ t ha}^{-1}$*
40 *y^{-1}). 20% of the total drainage area showed a critical value of SSY ($>10 \text{ t ha}^{-1} \text{ y}^{-1}$). The effects of different*
41 *fire-severity levels were analysed for one year after the fire, acting on a limited area (2.3% of the total basin*
42 *area). At the basin scale, the post-fire effect on surface runoff was negligible for all scenarios ($< 0.4\%$), and*
43 *the impact on SSY increased from $5.86 \text{ t ha}^{-1} \text{ y}^{-1}$ up to $12.05 \text{ t ha}^{-1} \text{ y}^{-1}$. At the subbasin scale, the post-fire*
44 *logging scenario showed the highest increase of soil loss (SSY increased from $9.48 \text{ t ha}^{-1} \text{ y}^{-1}$ to $57.40 \text{ t ha}^{-1} \text{ y}^{-1}$*
45 *y^{-1}). Post-fire mitigation treatments like straw mulching and erosion barriers effectively reduced soil erosion*
46 *in high- and moderate-severity fires ($19.12 \text{ t ha}^{-1} \text{ y}^{-1}$ and $20.93 \text{ t ha}^{-1} \text{ y}^{-1}$, respectively). At the hydrological*
47 *response unit level, the SSY estimated for the forest in the baseline ranged from $1.18 \text{ t ha}^{-1} \text{ y}^{-1}$ to $2.04 \text{ t ha}^{-1} \text{ y}^{-1}$*
48 *y^{-1} . It increased more than one order of magnitude for the high-severity fire scenarios and ranged from 4.33 to*
49 *$6.74 \text{ t ha}^{-1} \text{ y}^{-1}$ in the very low-severity fire scenario, underlining the scale effect from the HRU to the basin*
50 *scale.*

51 **Keywords:** forest fires, sediment yield, runoff, SWAT model, fire severity, post-fire mitigation measures

1. Introduction

The Mediterranean European Region is a high fire risk area due to a combination of several factors. The high number of buildings has increased the probability of fire ignition by human causes (Ganteaume et al., 2013) and, the abandonment of some rural areas has led to an accumulation of fuel loads that have contributed to fire ignition and spread, especially in summer (San-Miguel-Ayanz et al., 2012). Consequently, many fire events are recorded every year in this region (Fernández-Anez et al., 2021). San-Miguel-Ayanz et al. (2012) estimated that, in Europe, around 65000 fire events occur every year, burning about half a million hectares of forest. The European Environmental Agency (European Commission, 2019) pointed out that the burnt area in the Mediterranean region has shown a slight decrease since 1980. However, in the same period, the meteorological fire hazard has increased due to climate change.

Several researchers pointed out that droughts and high temperatures promote large fires in southern Europe (Camia and Amatulli, 2009; Lasaponara et al., 2018; Urbietta et al., 2015) and are also related to antecedent climate variables (Ruffault et al., 2016). Turco et al. (2017) highlighted that rising temperatures and droughts, which greatly influence summer fires, could make all fire prevention efforts useless in the next decades.

Wildfires may result in serious economic, cultural, and ecological damages in the Mediterranean Region (Ganteaume et al., 2021). A forest fire is a disturbance for the ecosystem; it may alter soil properties (Mataix-Solera et al., 2011; Lucas-Borja et al., 2018), reduce infiltration capacity and increase the peak of streamflow (Cerdà, 1998; Neary et al., 2005; Shakesby and Doerr 2006), ultimately changing the catchments hydrological and sedimentary processes (García-Comendador et al., 2017; Ice et al., 2004; Zema, 2021).

Wildfires seriously increase soil erosion (Fernández and Vega, 2018; Viera et al., 2015) and impair surface water quality by delivering fire-related contaminants to rivers with (Nunes et al., 2017; Verkaik et al., 2013; Campos et al., 2012; Chessman, 1986; Olivella et al., 2006). Fire severity (amount and duration of subsurface heating), nature of vegetation cover, physical and chemical characteristics of burnt areas (i.e. climate, soil, topography), and the time interval between the fire and rainfall determine the degree of impact on soil erosion and water quality (Viera et al., 2015; Teclé and Neary, 2015). Post-rehabilitation measures are needed to mitigate the effects of fire on hydro-sedimentary response and protect soil from erosion (Lucas-Borja, 2021). An accurate prediction of post-fire runoff and sediment yield is required to guide post-

80 fire risk management and plan soil and water restoration measures (Argentiero et al., 2021; Fernández et al.,
81 2010).

82 Hydrological and soil erosion models can provide valid support (Kampf et al., 2020) for quantifying the
83 catchment hydro-sedimentary response to forest fire events and planning adequate restoration measures.
84 Several modelling applications conducted to support management agencies are reported in the literature
85 (Lopes et al., 2021). The Revised Universal Soil Loss Equation (RUSLE) was applied to sites affected by
86 fire in the Mediterranean Region to estimate the impact on runoff and soil erosion (Coschignano et al., 2019;
87 Efthimiou et al., 2020; Fernández et al., 2010; Lanorte et al., 2019; Rulli et al., 2013). Analogously, the Pan-
88 European Soil Erosion Risk Assessment model (PESERA, Kirkby et al., 2004) was applied in central
89 Portugal (Esteves et al., 2012), Spain (Fernández and Vega, 2016), and Greece (Karamesouti et al., 2016).
90 The Water Erosion Prediction Project model (WEPP; Flanagan and Nearing, 1995) was used in Spain
91 (Fernández and Vega, 2018). Rulli and Rossi (2005; 2007) developed a distributed hydro-geomorphological
92 model to estimate the dynamics of fire-disturbed conditions at the basin scale. Di Piazza et al. (2007) used
93 the RUSLE model and a spatial disaggregation criterion for sediment delivery processes (SEDD model) to
94 assess the effects of bushfires in Italy. The Soil and Water Assessment Tool model (SWAT, Arnold et al.,
95 1998) was applied in two Portuguese sites to estimate the post-fire impacts on streamflow and sediment yield
96 (Basso et al., 2020; Nunes et al., 2018). Grangeon et al. (2021) proposed the WaterSed model to simulate
97 forest fire and firebreak scenarios and analyse their respective effects on sediment loads. Zema et al. (2020)
98 adapted the Morgan-Morgan-Finney model after wildfires in Spain. However, Lopes et al. (2021) pointed out
99 in their review that many of the published studies reported modelling applications without field validation
100 and that mitigation measures were simulated in a limited number of cases. The authors concluded that further
101 studies and tests were needed for adapting models to burnt conditions. Indeed, the model parametrisation is
102 not specifically designed for post-fire conditions, it needs to be adapted to the post-fire conditions, and
103 currently, it remains an open problem.

104 In this context, the present paper contributes to bridging the gap in modelling post-fire impact and
105 quantifying mitigation measures' effects. The general aim of the work is to test and adapt the SWAT model
106 as a tool for rapid post-fire erosion risk assessment. The specific aims of this work are: (i) to simulate runoff
107 and sediment yield for the current land use in a mountainous river basin, (ii) to predict the effects of forest

108 fire on runoff, erosion, and sediment transport, and iii) to quantify the effects of post-fire mitigation
109 measures on runoff and sediment yield at the basin, subbasin, and hydrologic response unit (HRU) scale.
110 Field measurements were used to calibrate the hydro-sedimentary parameters of the model for the current
111 land use in the Celone (S-E Italy) river basin that is characterised by an intermittent river network feeding
112 the Capaccio reservoir. The post-fire scenarios were simulated by changing the appropriate parameters
113 affecting hydrological processes and soil erosion by water. Simulated sediment yield and streamflow were
114 examined for the post-fire scenarios, including mitigation measures, and compared with the pre-fire
115 conditions to provide useful post-fire management information (i.e. quantification) to the river basin
116 managers.

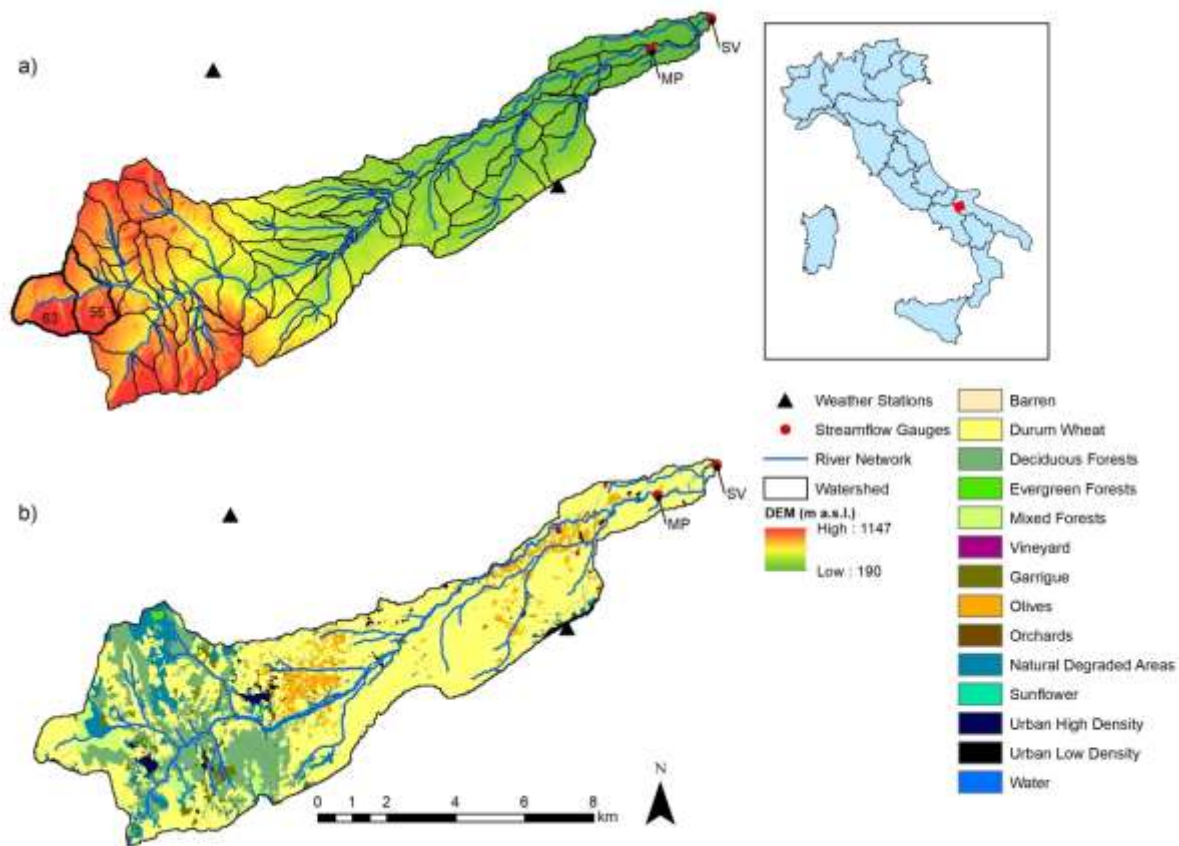
117 **2. Materials and methods**

118 **2.1 Study area**

119 The Celone River basin is located in northern Apulia (SE, Italy). The study area (72 km²) is located upstream
120 of the Capaccio reservoir (41° 25' 35''N; 15° 24' 52''E) (25.82 Million of m³), of which the Celone river is
121 the main inflow.

122 The elevation of the study area ranges from 1142 m a.s.l. to 218 m a.s.l. (mean value 386 m a.s.l.). Steep
123 slopes characterise the upper part of the basin, making it prone to erosion. The main channel is incised in the
124 mountainous area. Consequently, many check dams have been built to reduce bank erosion. Most of the
125 coarse material is deposited in the first alluvial plain, resulting in a braided river. Downstream, it continues
126 with a meandering pattern.

127 The lithology consists of flyschoidal units (flysch della Daunia), grey-blue clays in the mountain, and
128 alluvial deposits in the valley. The soils show a variable texture (clay, clay-loam, and sandy-clay-loam) and
129 is classified as typic-haploxerroll, vertic-haploxerroll, and typic-calcixerroll, according to the US Department
130 of Agriculture classification.



131

132 **Figure 1. Study area: Celone river basin (Apulia Region, Italy). a) DEM and subbasins distribution, subbasins**
 133 **affected by forest fire are delineated with continuous black lines (55, 63); b) Land use, gauging stations: MP**
 134 **(discharge and suspended sediment during the period 2010-2011), SV (discharge during the period 1994-1996).**

135

136 Mean annual rainfall is 770 mm (1990-2011), and mean temperature varies between 3.4°C (January) and
 137 20.3°C (August) in the mountain, and between 7.2°C (January) and 25.5°C (August) in the valley (De
 138 Girolamo et al., 2017a).

139 The soil erosion by water in the basin is both distributed (sheet erosion) and localised (rill erosion) (De
 140 Girolamo et al., 2015). It is favoured by agricultural practices such as conventional tillage (multiple
 141 operations with chisel plough and disks). The prevalent land use is for cereal growth (mostly winter and
 142 durum wheat; 45% of the catchment area). Other land use includes sunflowers (9%), natural degraded areas
 143 (6%), olive groves (8%), vineyards and vegetables (2%), and urban areas (1%). Forests, primarily oaks and
 144 conifers (29%), cover the mountainous part of the basin.

145 The study area was monitored in 2010-2011 at the Celone Masseria Pirro gauge (41°23'41''N; 15°20'02''E)
 146 (MP in Figure 1), with continuous measurements of streamflow and discrete suspended sediment

147 concentration samples (De Girolamo et al., 2015; De Girolamo et al., 2018). Daily streamflow was computed
148 starting from measurements taken on 15-min of the time step, and suspended sediment load at the monthly
149 time scale was estimated using the sediment rating curve developed based on measured streamflow and
150 suspended sediment concentrations (Eq. R3 in De Girolamo et al., 2018).

151

152 **2.2 Conceptual model**

153 The SWAT model with ArcGIS interface (Arnold et al., 1998) was used in the present work to simulate
154 streamflow and sediment yield and predict the potential impact of forest fire and post-fire measures on
155 sediment and hydrology. SWAT is a semi-distributed model able to predict hydrological processes, water
156 quality, and the environmental impact of land use and management practices on water bodies and soils in
157 agricultural basins (D'Ambrosio et al., 2020a; De Girolamo and Lo Porto, 2020). The SWAT model is
158 widely used for assessing the effects of anthropogenic pressures on water quality (Cakir et al., 2020;
159 D'Ambrosio et al., 2020b; Pulighe et al., 2019) for estimating climate change impact on water resources and
160 flow regimes (Brouziyne et al., 2020), and for simulating soil erosion (Vigiak et al., 2017; Gamvroudis et al.,
161 2015) and the impact of best management practices (BMPs) on water resources (Ricci et al., 2020).

162 In SWAT, the basin is divided into subbasins that are further subdivided into HRUs, which are characterised
163 by homogeneous land use, soil, and slope. The water cycle is divided into the land phase and routing phase.
164 The components of the land phase (i.e. runoff, evapotranspiration, crop growth, soil erosion, nutrient and
165 pesticides loads entering into the main channel) and the methods used for their computation are described in
166 Neitsch et al. (2011). The routing phase through the river network includes transmission losses and
167 degradation of nutrients, pesticides, and bacteria. Similarly, the sediment budget is divided into two
168 components, landscape phase and channel routing. The soil erosion phase includes the detachment, transport,
169 and deposition of soil particles by the erosive force of raindrops and the surface flow of water. The channel
170 sediment routing phase considers deposition and degradation that occurs in the channel. The landscape
171 sediment phase is computed with the modified universal soil loss equation (MUSLE), and the channel
172 sediment routing is computed using the Bagnold equation (Neitsch et al., 2011). The SWAT model provided
173 outputs at the basin, subbasin, and reach scale.

174 The model was run at a daily time step from 1990 to 2011. The Hargreaves-Samani equation was selected for
 175 estimating the potential evapotranspiration (PET), and the SCS Curve Number Method was adopted to
 176 calculate surface runoff (Neitsch et al., 2011). Table I summarises input data used in the present study, their
 177 source, and resolution.

178
 179

Table I. Input data: variable, origin, scale, information.

Variable	Origin	Scale	Information
Precipitation	Civil Protection Service Apulia Reg. Agency	Daily	2 weather stations (1990-2009)
Temperature	Civil Protection Service Apulia Reg. Agency	Daily min, daily max	2 weather stations (1990-2009)
Land use map	Corine Land Cover 2000 EU Project	ArcInfo format (scale 1:100000)	Minimum area digitalized 25 ha
Soil map	ACLA 2 - FEOGA EU Project	ArcInfo format (scale 1:100000)	5 soil profiles
Management Practices	Consorzio per la Bonifica della Capitanata; farmers	Subbasin scale; Municipality	Tillage oper., irrigation amount, fertilizers appl. (timing, amount)
Digital Elev. Model	Apulia River Basin Authority	Arc Info grid format (8x8m)	

180

181

2.3 Model calibration

182 The sensitive analysis, reported in De Girolamo et al. (2017a), identified among the most sensitive
 183 parameters influencing hydrological processes the initial SCS curve number for moisture condition II (CN2),
 184 the threshold depth of water in the shallow aquifer required for return flow to occur (GWQMN [mm]), the
 185 available water capacity of the soil layer (SOL_AWC [mmH₂O/mmsoil]), the soil evaporation compensation
 186 factor (ESCO), the surface runoff lag time (SURLAG [days]), revap coefficient (GWREVAP), the Baseflow
 187 alpha-factor (ALPHA_BF, [days]), and Groundwater delay time (GW_DELAY, [days]).

188 In the present study, the model SWAT2012 version was used. The basin was divided into 74 subbasins,
 189 further partitioned into 200 HRUs. Conservation practices were not adopted in the study area (Panagos et al.,
 190 2015a; Wischmeier and Smith, 1978). The conservation practice factor (USLE_P) was assumed to be equal
 191 to 1 for all land uses, except for forested areas where the P factor was set to 0.8. According to the crop
 192 systems, the crop management factor (USLE_C) was set within 0.0019 to 0.2, as suggested by Panagos et al.
 193 (2015b).

194 The model was calibrated for the streamflow at the SV gauge over 1994-1996 and at the MP gauge over
 195 2010-2011 (Figure 1). The sediment load was calibrated at the MP gauge (2010-2011), and the validation
 196 was carried out for streamflow at the SV gauge (1992). Manual calibration was performed, including the
 197 above-mentioned parameters for hydrology. For sediment load calibration, the following parameters were

198 included: channel erodibility factor (CH_COV1), channel cover factor (CH_COV2), Manning's "n" value
 199 for the main channel (CH_N2), the maximum amount of sediment that can be transported from a river reach
 200 (SPCON), and the exponent for calculating sediment that can be transported in the channel (SPEXP). Table
 201 II shows the parameter values corresponding to the best fit for the most sensitive parameters and their range
 202 of variability.

203 The model's performance was evaluated by using the coefficient of determination (R^2), the Nash-Sutcliffe
 204 efficiency (NSE), and the observation standard deviation ratio (RSR). The simulations were considered good
 205 if $0.65 < NSE < 0.75$, $0.5 < RSR < 0.6$ and $R^2 > 0.8$ and satisfactory if $0.5 < NSE < 0.65$, $0.65 < RSR < 0.7$
 206 and $R^2 > 0.5$ (Moriassi et al., 2007).

207 **Table II. Calibrated parameters (actual value used) and their range of variability.**

Parameter	Description	Actual value used	Range
CN2	SCS Curve number for moisture condition II	70-85 ^a	35-98
GWQMN	Threshold depth of water in the shallow aquifer required for return flow to occur [mm H ₂ O]	800	0-5000
OV_N	Manning's "n" value for overland flow	0.1-0.4 ^a	
SOL_AWC	Available water capacity [mm H ₂ O/mm soil]	0.12-0.21 ^a	0-1
ESCO	Soil Evaporation compensation factor	0.95	0-1
SURLAG	Surface runoff lag coefficient [days]	2	0-10
GWREVAP	Revap coefficient	0.02	0.02-0.2
ALPHA_BF	Baseflow alpha factor [days]	0.95	0-1
GW_DELAY	Groundwater delay time [days]	3	
CH_N2	Manning's "n" value for main channel	0.11	0.05-0.5
CH_COV1	Channel erodibility factor	0-0.5 ^b	0-1
CH_COV2	Channel cover factor	0-5 ^b	0-1
SPCON	Maximum amount of sediment retrained during channel sediment routing	0.007	0.0001-0.01
SPEXP	Exponent for calculating sediment retrained in channel	1.8	1-2

208 ^a value varies according to input data (soil, land use)

209 ^b value = 0 was assumed for reaches in plain area; values > 0 was assumed in the mountainous and hilly reaches.

210

211 2.4 Analysis at the reach scale

212 After the fire events, the sediment-associated pollutants transported via surface runoff could accumulate on
 213 the riverbed with several implications on water quality and ecological status. In order to identify the river
 214 segments where the deposition of sediment occurs, an analysis at the reach scale was carried out for the
 215 period 1990-2011. Thus, the sediment transported with water into the reach (SED_IN) were combined with
 216 the sediment transported with water out of the reach (SED_OUT), and the sediment from the subbasin to the
 217 river reach during the time step to identify the river reach's under erosion and deposition.

218 2.5 Simulating post-fire scenarios

219 Post-fire scenarios were simulated assuming that fire burnt the forest areas in two selected subbasins [Figure
220 1, Numbers 55, 63]. The basins were selected to analyse the effect of fire severity and management in soil
221 erosion-prone areas. Both subbasins were characterised by steep slopes, high rainfall, and soil erodibility.
222 The drainage area of subbasin 55 was 2.09 km², 1.17 km² was covered by forests, and the drainage area of
223 subbasin 63 was 2.47 km², including 0.47 km² covered by forests. The fire was assumed to occur in 2010
224 only in forested areas.

225 The post-fire scenarios and the effectiveness of selected mitigation measures in reducing soil erosion by
226 water were analysed for one year after the fire. Mayor et al. (2007) and Pausas et al. (2008) pointed out that
227 soil erosion might be two orders of magnitude higher five years after the fire. However, the highest
228 hydrological and erosive events occur beyond the first year after the fire (García-Comendador et al., 2017).
229 The following six scenarios were simulated to provide a wide range of potential impacts on hydro-
230 sedimentary response to support post-fire management. The model parameters influencing runoff and soil
231 erosion were properly modified for each scenario using literature values. Table III shows the parameters and
232 their values for the baseline and post-fire scenarios and the most relevant references used as guides for their
233 selection and values' attribution.

234

235 *Scenario Fr1: high-severity fire and post-fire logging*

236 It was assumed that “high-severity fire” was ground and canopy fire (all shrubs and herbaceous plants killed)
237 with high soil heating and alteration of soil structure (decreased infiltration and increased water repellency).
238 This scenario analysed the potential effect of removing fire-killed trees from burnt areas (logging) and the
239 successive tillage operation (chisel plough) on those areas.

240 The fire effect on soil characteristics was simulated by modifying the USLE erodibility factor (USLE_K).
241 The effect of fire on soil water repellency (Sol_K) was incorporated into the USLE_K by adopting the
242 suggestions by Miller et al. (2003) (reported by Larsen and MacDonald, 2007). The reduction of soil
243 protection due to the damage of vegetation cover was considered by modifying USLE_C. In literature, the
244 post-fire USLE_C factor applied ranges from 0.01 (low severity) to 0.3 (high severity) (Borrelli et al., 2016).

245 USLE_P was set equal to one, and the increase of runoff at the different spatial scales consequent to the fire
246 events were estimated by modifying OV_N and the CN2 (Table III).

247

248 *Scenario Fr2: high-severity fire and natural regeneration*

249 High-severity fire impact on soil was simulated by increasing the USLE_K (Table III). For this scenario,
250 USLE_P was set to 1, and USLE_C was fixed to 0.13 to mimic the effect of the regrowth of vegetation. CN2
251 was increased (+15) compared to the baseline scenario (Havel et al., 2018). Meanwhile, OV_N was assumed
252 lower than the baseline (Table III).

253

254 *Scenario Fr3: high-severity fire and emergency stabilisation (straw mulching and seeding)*

255 Straw mulching was considered in this scenario to protect soil after the fire. The effect of straw mulching
256 was simulated by modifying USLE_P, USLE_C, CN2, and OV_N. USLE_P was set to 0.343 and USLE_C
257 to 0.13, considering the effect of seeding and regrowth of vegetation (Fernandez et al., 2010; and Rulli et al.,
258 2013). In addition, mulch material on soil is a conservation practice that is generally simulated by modifying
259 the CN2; here, it was reduced by 3 points compared to the value assigned in Fr2 (Waidler et al., 2009).
260 Finally, OV_N was increased compared to Fr1 and Fr2, but lower than the one assumed in the baseline, as
261 suggested by Neitsch et al., 2011.

262

263 *Scenario Fr4: moderate-severity fire and erosion barriers*

264 In this scenario, the moderate-severity fire was hypothesised, and erosion barriers were simulated as a post-
265 fire mitigation measure to reduce surface runoff and soil losses. The assumption was ground fire and burning
266 of lower tree limbs, moderate soil heating, increased water repellency and decreased infiltration. The
267 baseline value of USLE_K was assumed to increase (Table III), and OV_N and CN2 were reduced and
268 increased, respectively. USLE_P was modified by adopting the value of 0.85 (Myronidis et al., 2010).
269 Nevertheless, it is important to underline that literature reports a wide range of USLE_P values applied (from
270 0.2 to 0.85).

271

272 *Scenario Fr5: low-severity fire and natural regeneration*

273 Low-severity fire and natural regeneration were simulated in this scenario. It was assumed that leaf litter was
 274 completely consumed with small changes in soil properties. All the parameters mentioned above were
 275 modified as reported in Table III. OV_N was assumed to be 0.3, and the baseline value of CN2 was
 276 increased (+5), USLE_K was assumed to increase to a lesser extent than moderate-and high-severity fire.

277

278 *Scenario Fr6: very low-severity fire and natural regeneration*

279 In this scenario, it was assumed that fire had very lightly charred only fine fuel and litter on the ground and
 280 soil properties (i.e. hydraulic saturated conductivity, water repellency) were unchanged. The baseline value
 281 of CN2 was slightly increased (+3), and USLE_K was unchanged (Table III).

282 **Table III. SWAT parameters used in the baseline simulation and fire scenarios.**

Parameter	Description	Baseline	Fr1 High-severity fire, logging, tillage	Fr2 High-severity fire, natural regeneration	Fr3 High-severity fire, straw mulching and seeding	Fr4 Moderate-severity fire and erosion barriers	Fr5 Low-severity fire and natural regeneration	Fr6 Very low-severity fire and natural regeneration	Reference
OV_N	Manning's roughness coefficient	(0.4)	0.09 ^a	0.16 ^{a,b}	0.22 ^a	0.25 ^a	0.3 ^a	0.3 ^a	^a Neitsch et al., 2011; ^b Stoof et al., 2015
USLE_P	USLE eq. supporting practice factor	0.8 ^{a,b}	1	1	0.343 ^{c,d}	0.85 ^{d,e}	0.9	0.9	^a Panagos et al., 2015a; Wischmeier and Smith, 1978; ^c Fernandez et al., 2010; ^d Rulli et al., 2013; ^e Myronidis et al., 2010.
USLE_C (m ² /m ²)	USLE C factor for water erosion	0.0019 ^a	0.23 ^b	0.13 ^{c,d}	0.13 ^{c,d}	0.05 ^{e,f}	0.01 ^{e,f}	0.01 ^{e,f}	^a Panagos et al., 2015b; ^b Fernandez et al., 2016; ^c Fernández & Vega, 2018; ^d Rulli et al., 2015; ^e Larsen and MacDonald, 2007; ^f Terranova et al. 2009.
CN2	Initial SCS runoff curve number for soil moisture condition II	(70)	90 ^a	85 ^b	82 ^{b,c}	80 ^{b,d}	75 ^{b,d}	73	^a Neitsch et al., 2002; ^b Havel et al., 2018; ^c Waidler et al., 2009; ^d Basso et al., 2020.
USLE_K* (ton acre hour)/(hundred acre ft ton inch)	USLE eq. Soil erodibility factor	0.13-0.15	+0.016/0.1317 ^{a,c,d}	+0.016/0.1317 ^a	+0.016/0.1317 ^a	+0.015/0.1317 ^b	+0.014/0.1317 ^c	0.13-0.15 ^c	^a Miller et al., 2003; ^b Fernandez et al., 2010; ^c Basso et al., 2019; ^d Coschignano et al., 2019; ^e Di Piazza et al., 2007.
Tillage	Plowing (chisel)		Deep						Nunes et al., 2018.

	plow)								
--	-------	--	--	--	--	--	--	--	--

283 *0.1317 is the conversion factor for soil erodibility factor (USLE_K) from t h MJ⁻¹ mm⁻¹ to ton acre hour/ hundred acre ft ton inch

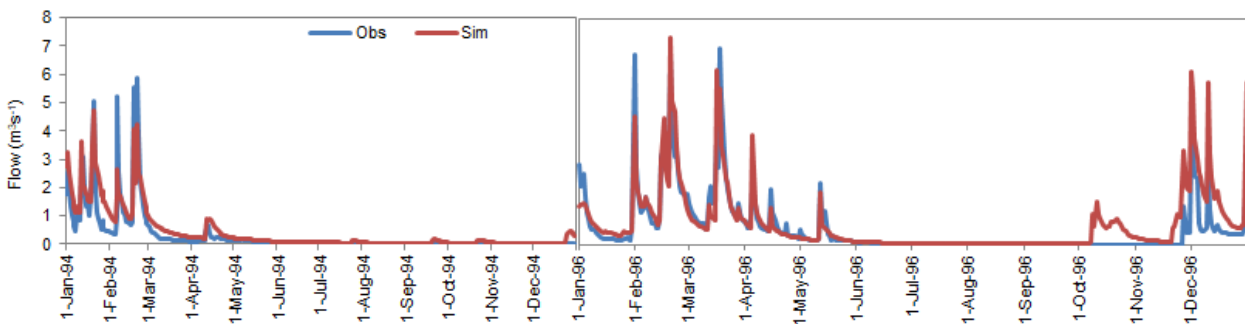
284

285 3. RESULTS

286 3.1 Modelling streamflow and sediment load

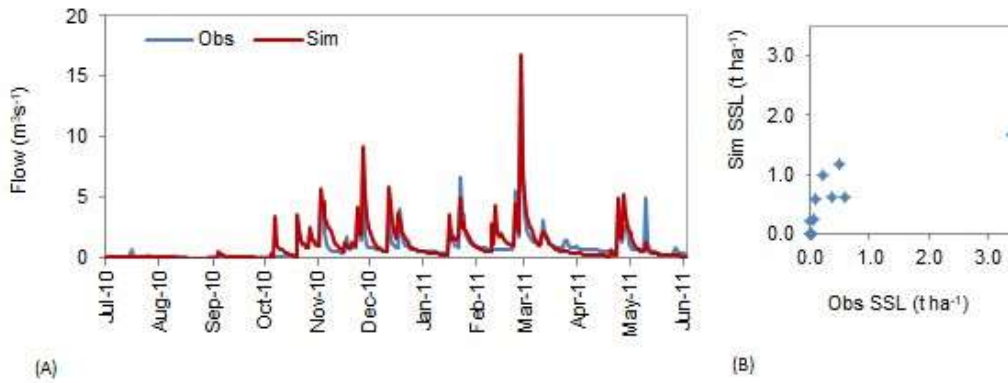
287 The statistics obtained for daily streamflow calibration showed a good model efficiency at the SV gauge
 288 (NSE = 0.70; RSR = 0.54; R² = 0.88) and at the MP gauge (2010-2011) (NSE = 0.73; RSR = 0.50; R² =
 289 0.89). Similar results were obtained for the validation period of the streamflow at the SV gauge (NSE = 0.73;
 290 RSR = 0.63; R² = 0.90). Figure 2 shows the simulated and observed streamflow for the calibration period at
 291 the SV gauge. The performance for sediment calibration on the monthly time scale at the MP gauge was
 292 satisfactory (NSE = 0.73; RSR = 0.70; R² = 0.54). The results showed an underestimation of sediment load
 293 in March 2011, when a series of large floods occurred, and an overestimation in autumn. Figure 3 shows the
 294 observed and simulated daily streamflow at the MP gauge (Figure 3A) and monthly observed specific
 295 sediment load (SSL, t ha⁻¹) versus simulated values (Figure 3B).

296



297
 298 **Figure 2. Simulated and observed streamflow for the calibration period at the SV gauge.**

299



300
301
302
303
304

Figure 3. Observed and simulated daily streamflow at the MP gauge (A). Measured versus simulated specific sediment load SSL (t ha^{-1}) at monthly time scale for the calibration period (2010-2011) (B).

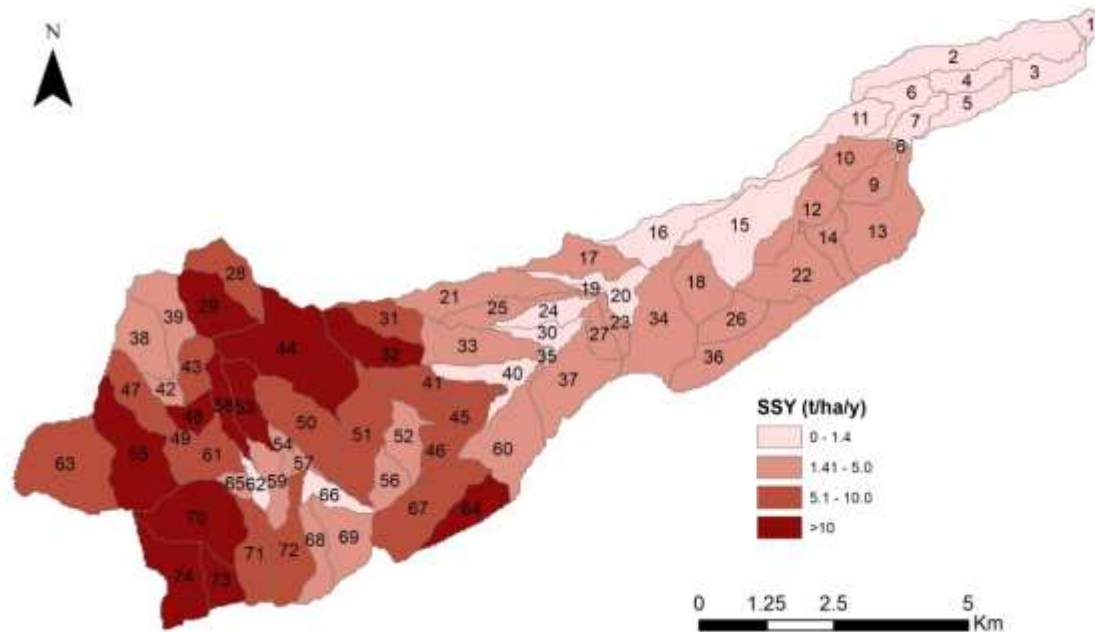
305

3.2 Streamflow and sediment load for the current land use (baseline)

306

At the basin scale, from 1990 to 2011, the average annual rainfall was 777 mm (SD = 179 mm), mainly concentrated from November to April (wet season), the surface runoff was 114 mm (SD = 66 mm), and the total water yield was 288 mm (SD = 140 mm). Most of the rainfall (61%) was lost via actual evapotranspiration (471 mm; SD = 41 mm), and the potential evapotranspiration was 954 mm (SD = 30 mm). The average annual SSY (sediment yield per unit of catchment area and unit of time; $\text{t ha}^{-1}\text{y}^{-1}$) was $5.60 \text{ t ha}^{-1} \text{ y}^{-1}$ (SD = $3.47 \text{ t ha}^{-1} \text{ y}^{-1}$). A high inter-annual variability characterised all the water balance components and the SSY due to differences in climate conditions. In the driest year (2000), the total annual rainfall was 471 mm, surface runoff (SR) was about 26 mm, and the SSY was $3.03 \text{ t ha}^{-1} \text{ y}^{-1}$. In the wettest year (2009), the total annual rainfall was 1217 mm, SR was 300 mm, and SSY was $13.82 \text{ t ha}^{-1} \text{ y}^{-1}$.

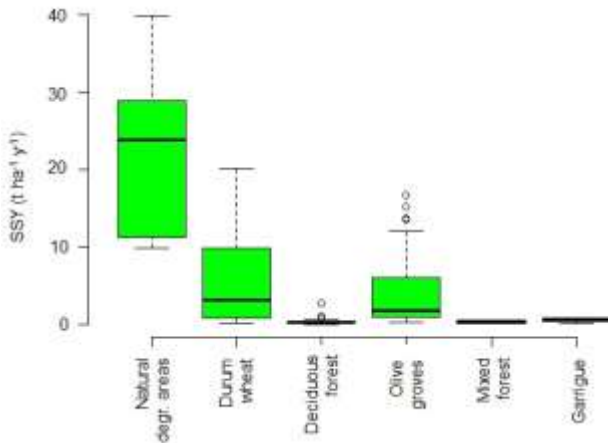
314



315
 316
 317
 318
 319
 320
 321
 322
 323
 324
 325
 326
 327
 328
 329
 330

Figure 4. Average specific sediment yield (SSY, t ha⁻¹ y⁻¹) at the subbasin scale estimated from 1990 to 2011.

At the subbasin scale (Figure 4), over the period 1990-2011, the mean annual SSY was < 1.4 t ha⁻¹ y⁻¹ in the subbasins located in the plain area (14% of total drainage area). Most of the subbasins showed values between 1.4 to 10 t ha⁻¹ y⁻¹, and some mountainous subbasins (20% of total drainage area)—characterised by steep slopes—showed severe soil erosion (SSY > 10 t ha⁻¹ y⁻¹). These results are consistent with the new assessment of soil loss by water erosion in Europe performed with the RUSLE2015 by Panagos et al., 2015c. At the HRU level, natural degraded areas, predominant in the steep slopes areas, showed the highest values of SSY. Also, durum wheat fields, where up-and-down tillage was generally adopted, showed high values of SSY. Garrigue, deciduous, and mixed forests showed lower values of SSY. The box plot in Figure 5 shows the annual SSY estimated at the HRU level for each crop. Wide variability was found among the HRUs for each crop because of the different environmental factors (slope, soil, rainfall) that influence hydrology and soil erosion.



331
332
333

Figure 5. Box plot of the average specific sediment yield (SSY, $\text{t ha}^{-1} \text{y}^{-1}$) estimated at the HRU level from 1990 to 2011. The horizontal line within the box plot indicates the median, boundaries of the box indicate the 25th and 75th percentile, and whiskers indicate the minimum and maximum values.

337

The reach-scale analysis for identifying the river segments where sediment deposition occurs showed that

339

most first-order river segments were under erosion. Meanwhile, sediment deposition was predicted in some

340

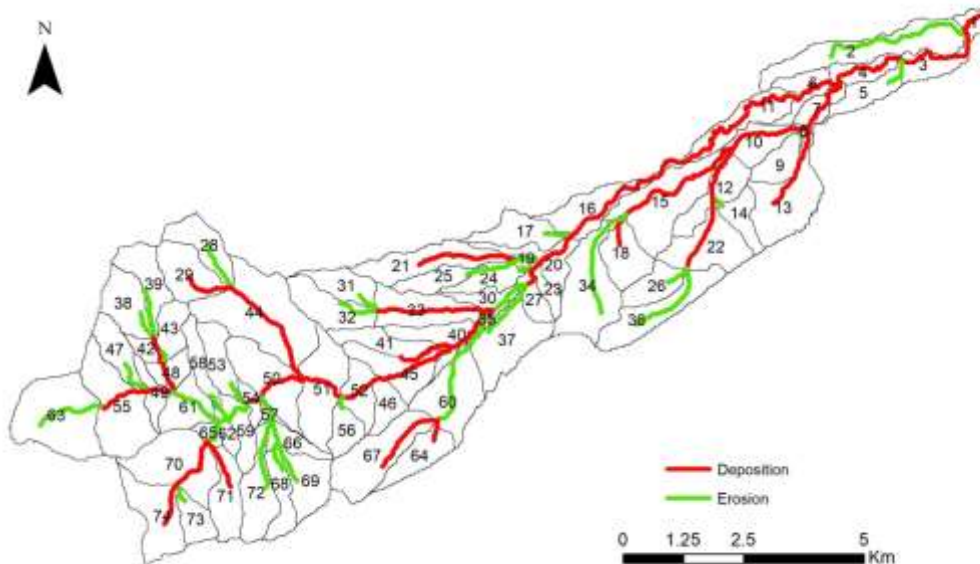
intermediate reaches and those located in the alluvial plains (Figure 6). In the latter, if fire events occur in the

341

upstream areas, pollutants such as Fe, Mn, As, Cr, Al, Ba, and Pb could be deposited along the river bed, and

342

the water quality could be impaired (Smith et al., 2011).



343
344

Figure 6. Segments of the Celone River under erosion and deposition.

345

3.3 Post-fire scenarios: potential impact on hydro-sedimentary response

346

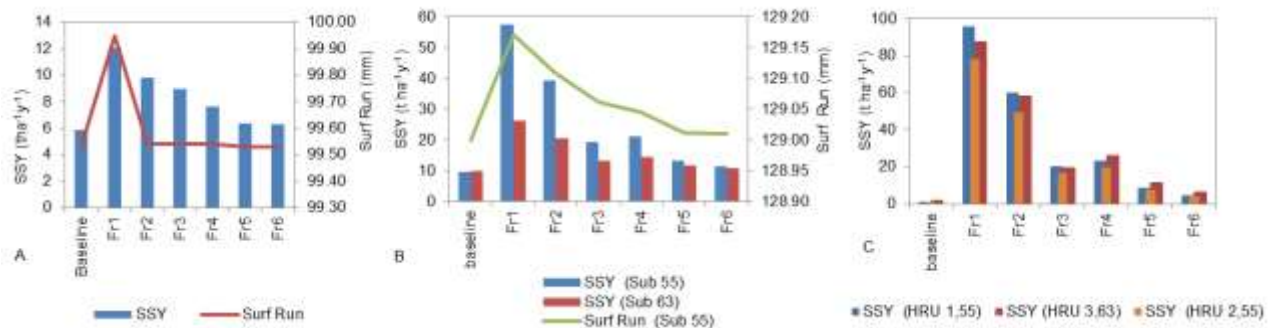
At the basin scale, the integrated effect of the two burnt areas (1.64 km^2 , 2.3% of the entire river basin) on

347

surface runoff was negligible. Only the scenario Fr1 showed a slight increase in annual surface runoff (99.95

348 mm) compared to the baseline (99.53 mm) (Figure 7A). Similarly, the impact of wildfire on the total water
 349 yield (total streamflow at the outlet for the unit area; TWY, mm) was negligible for all the scenarios. The
 350 lateral flow and baseflow contributions to the streamflow showed a slight decrease only for Fr1 (194.56 mm)
 351 compared to the baseline (194.88 mm). It can be inferred that these results depend on the limited extension
 352 of the burnt area (2.3%). For all the fire scenarios, including post-fire mitigation measures, an increase in
 353 SSY was modelled, ranging from 5.86 t ha⁻¹ y⁻¹ (baseline) to 12.05 t ha⁻¹ y⁻¹ (Fr1) (Figure 7A). The severity
 354 of the fire played an essential role in SSY. A massive difference was predicted between high-severity fire
 355 (Fr1 and Fr2) and low-severity fire scenarios (Fr5, Fr6, Figure 7A). Fr5 and Fr6 showed limited increases in
 356 SSY (6.4 and 6.3 t ha⁻¹ y⁻¹) compared to the baseline. The post-fire management decreased SSY compared to
 357 Fr1 (8.9 t ha⁻¹ y⁻¹ and 7.7 t ha⁻¹ y⁻¹ for Fr3 and Fr4, respectively), although it was still higher than the baseline
 358 (Figure 7A).

359



360

361 **Figure 7. Specific sediment yield (SSY, t ha⁻¹ y⁻¹) and surface runoff simulated for the baseline and post-fire**
 362 **scenarios at the basin scale (A), subbasin scale (B), and at the hydrological response unit level (HRU) (C).**

363

364 Results at the subbasin scale showed negligible variations in surface runoff (ranging from 129.01 mm to
 365 129.17 mm) for all the analysed scenarios in the subbasin 55 (Figure 7B) compared with the baseline (129.00
 366 mm). Similarly, the increase in surface runoff simulated for the subbasin 63 was negligible, ranging from
 367 98.78 mm (baseline) to 98.83 mm (Fr1), and for low-severity fire simulated in the Fr5 and Fr6 scenarios, it
 368 was 98.79 mm. The SSY simulated for the baseline (9.5 t ha⁻¹ y⁻¹ and 9.7 t ha⁻¹ y⁻¹, for sub 55 and sub 63,
 369 respectively) increased up to 57.4 t ha⁻¹ y⁻¹ (sub 55, Fr1) and up to 26.1 t ha⁻¹ y⁻¹ (sub 63, Fr1), confirming
 370 that the high severity of fire events and the post-fire logging may produce a dramatic increase in soil loss
 371 (Figure 7B). The extension of the burnt area within the basin played an essential role in SSY variations.
 372 Indeed, as a result of the larger burnt area in the subbasin 55 (56%), the SSY predicted in this subbasin was
 373 much more than SSY simulated in the subbasin 63 (burnt area 19% of subbasin area), especially in the high-

374 severity fire scenarios with no measures to reduce soil erosion (Fr1, Fr2) (Figure 7B). Post-fire mitigation
375 treatments (Fr3 and Fr4) effectively reduced soil erosion in high- and moderate-severity fires. In particular,
376 straw mulching and seeding—as simulated in Fr3—protected ground cover better than erosion barriers (Fr4)
377 (Figure 7B). Indeed, SSY was 19.11 t ha⁻¹ y⁻¹ and 13.13 t ha⁻¹ y⁻¹ (subbasin 55 and 63, respectively) in Fr3
378 and 20.93 t ha⁻¹ y⁻¹ and 14.35 t ha⁻¹ y⁻¹ (sub 55 and 63, respectively) in Fr4, while fire severity was simulated
379 to be high and moderate, respectively. As expected, due to the lower severity of fire represented by the Fr5
380 and Fr6, SSY increased to a lesser extent in these scenarios, ranging from 11.4 t ha⁻¹ y⁻¹ (Fr6) to 13.3 t ha⁻¹ y⁻¹
381 (Fr5) in the subbasin 55, and from 10.62 t ha⁻¹ y⁻¹ (Fr6) to 11.57 t ha⁻¹ y⁻¹ (Fr5) in the subbasin 63.
382 The analysis of the potential impact of post-fire scenarios in terms of soil erosion was carried out also at the
383 HRU level. Figure 7C shows the results for the three HRUs. The SSY estimated for the baseline ranged from
384 1.18 t ha⁻¹ y⁻¹ to 2.04 t ha⁻¹ y⁻¹. It increased more than one order of magnitude for the high-severity fire
385 scenarios, Fr1 ranged from 78.19 t ha⁻¹ y⁻¹ to 95.77 t ha⁻¹ y⁻¹ and Fr2 from 49.40 t ha⁻¹ y⁻¹ to 59.91 t ha⁻¹ y⁻¹.
386 As expected, the very low-severity fire scenario presented the lower increase of SSY, ranging from 4.33
387 (HRU 2,55) to 6.74 t ha⁻¹ y⁻¹ (HRU 3,63)(Figure 7C).

388 4. Discussion

389 4.1 Simulating baseline

390 Soil erosion models are widely used around the world for estimating soil losses by water (Borrelli et al.,
391 2021, Bezac et al., 2021), although some critical points have not been completely solved yet (i.e.
392 parameterisation, lack of measurements to validate results, upscaling from local to larger scales). The present
393 study shows that the SWAT model is a valuable tool to simulate both the hydrological processes and SSY
394 under the Mediterranean climate, and it has great potential in watershed management.

395 The model has already been successfully used in the Apulia Region (De Girolamo et al., 2017a,b) for
396 analysing hydrological processes. However, the low flow was generally overestimated. Similarly, in the
397 present work, the model did not simulate the zero-flow condition, which was recorded in the summer in
398 several observed years. The minimum flow predicted by the model was about 20 l s⁻¹. In the previously
399 mentioned studies, which were oriented to support ecological status evaluation, it was identified that a zero-
400 flow threshold and time series of streamflow were appropriately modified. In the present study, taking into

401 account that the extremely low flow is characterised by negligible sediment transport, the discrepancy
402 between observed and simulated streamflow was considered insignificant for the research.

403 The model performance in simulating SSY was satisfactory. Nevertheless, SSY was underestimated in the
404 extremely wet conditions and slightly overestimated in autumn, confirming the results obtained by
405 Abdelwahab et al. (2018), who implemented the SWAT model in the Carapelle basin (Apulia Region). Data
406 resolution and problems linked to the transferability of the Modified Universal Soil Loss Equation approach
407 may have influenced model performances (Ricci et al., 2018; Williams & Berndt, 1977).

408 At the basin scale, over the period 1990 to 2011 that included both dry and wet years, SSY was $5.60 \text{ t ha}^{-1} \text{ y}^{-1}$.
409 This estimate was comparable with the studies carried out in the same region by Ricci et al. (2018). At the
410 subbasin scale, SSY varied in the range $0.2\text{-}17.6 \text{ t ha}^{-1} \text{ y}^{-1}$. 20% of the total drainage area presented SSY
411 values higher than the critical value ($10 \text{ t ha}^{-1} \text{ y}^{-1}$). These results agree with the soil losses estimated by
412 Panagos et al. (2015c; 2016) and by Kirkby et al. (2004; 2008).

413 At the HRU's level, land use and management practices played a key role in determining SSY variations.
414 Natural degraded areas with a very low vegetation rate showed a very high SSY (median value $23.8 \text{ t ha}^{-1} \text{ y}^{-1}$),
415 mainly due to their location on steep slopes. Agricultural lands predominated by the basin's prevalent
416 crop—durum wheat—showed a median value of $3.2 \text{ t ha}^{-1} \text{ y}^{-1}$, comparable with the predicted soil loss rate
417 from erosion plots in Europe (Cerdan et al., 2010). Deciduous and mixed forests showed low SSY (0.3 t ha^{-1}
418 y^{-1}). These results were expected since it is well known that human activities such as agriculture and land-use
419 change have induced an important increase in erosion rates (Foucher et al., 2021; Poesen, 2018). In the study
420 area, soil losses are favoured by up and down ploughing, which is common, especially in mountainous areas.

421 It is important to remember that the dataset used for sediment calibration was limited and that measurements
422 taken at the outlet could be insufficient for optimal parameterisation. Hence, an uncertainty degree could
423 affect the results at the subbasin and HRU levels. In the present study, parameters such as USLE_P and
424 USLE_C were fixed on the literature basis and were not calibrated. A new monitoring plan with a nested
425 approach could be very useful for improving model parameterisation and SSY estimation.

426 Despite its limitations, the model can predict the hydro-sedimentary response of the basin and may
427 contribute to the management of the reservoir, providing both the inflow and sediment loads.

428 4.2 Simulating post-fire mitigation measures

429 The forest located in the upper Celone river basin is an important natural area, it has been recognised as a
430 Site of Community Importance, and it is included in the network “Natura 2000” (IT9110003) that covers
431 Europe’s valuable species and habitats. The Regional Plan 2018-2020 developed by the Civil Protection
432 Agency classified this area as a “high risk of fire” site due to weather conditions and ignition sources (Civil
433 Protection Agency, 2018). Future climate projections predict an increase in temperature and a reduction of
434 rainfall (De Girolamo et al., 2017b) that could increase the probability of wildfires and the risk of short and
435 long-term post-fire contamination for surface waters.

436 To manage the post-fire risks and select appropriate mitigation measures to reduce soil erosion, it is
437 necessary to know the effects of wildfire on hydrology and soil erosion (Zema, 2021) and analyse the effects
438 of different post-fire scenarios (Rulli et al., 2013). The present work tries to address these issues.

439 The hydro-sedimentary response of a watershed to fire events is complex (Vieira et al., 2018). It is related to
440 fire impact on soil properties and changes in the vegetation cover (Cerdà and Doerr, 2008; Neary et al., 1999;
441 Neary et al., 2005; Shakesby et al., 2011). The difficulties in evaluating the hydrological and sediment
442 regimes generally increase in the Mediterranean environment with intermittent river networks due to the high
443 spatial variability of soil properties, land use, and climate (Forteza et al., 2021).

444 The SWAT model, indispensable in water and soil management, may be used for the scenario analysis in the
445 context of wildfire, but it needs to be adapted. Indeed, SWAT and all other hydrological/soil erosion models
446 have not been developed specifically to simulate post-fire conditions. The adaptation consists of changing
447 hydrological, soil, and cover parameters in an attempt to mimic the effect of fire (Lopes et al., 2021). Then,
448 the model predictions should be calibrated, comparing the results with measurements. This is a critical point;
449 most studies have not been validated with field observations since the latter are rarely available, especially at
450 the basin scale (Lopes et al., 2021).

451 After fire events, land degradation and soil properties changes are not easy to measure and model since the
452 effect may change according to the severity of fire and characteristics of the soils (Neary et al., 1999).
453 Literature reports severe impacts on soil properties, providing sometimes conflicting results. Ice et al. (2004)
454 reported that reduction in infiltration rate could be very high (i.e. one or two orders of magnitude). Stoof et
455 al. (2015), in their study in Portugal, evaluated that despite the high fire intensity, bulk density, organic

456 matter, porosity, and saturated hydraulic conductivity did not significantly change. Nevertheless, they
457 concluded that even if the fire has a low impact on soil properties, it may have a high impact on runoff and
458 erosion. Mataix-Solera et al. (2011), in their review, reported that the effect on soil aggregate stability may
459 increase or decrease for similar fire-severity events according to the soil characteristics. Post-fire water
460 repellency, which is a key factor in post-fire erosion since it reduces infiltration rate, especially after high-
461 severity fires, is highly variable spatially (Doerr et al., 2009; Shakesby and Doerr, 2006) and difficult to
462 accurately estimate.

463 This work assumes that wildfire increases the soil's water repellency and reduces the saturated hydraulic
464 conductivity, except for the very-low fire (Fr6). A reduction of the soil protection consequent to damage of
465 vegetation cover was assumed to vary according to the scenarios. Hence, the effect of fire and the post-fire
466 mitigation measures on runoff and SSY was estimated by modifying parameters such as OV_N, CN2,
467 USLE_K, USLE_C, and USLE_P after an accurate literature analysis. To take into account the change in
468 water repellency (not explicitly considered in the models) and the consequent reduction of soil permeability,
469 it was assumed that an increase of USLE_K by $0.016 \text{ Mg ha}^{-1} \text{ MJ}^{-1} \text{ mm}^{-1} \text{ ha h}$, considering a high rate of
470 change in soil erodibility (60-80%) as suggested by Miller's et al. (2003).

471 Post-fire measurements were not available. Due to this, the model was not calibrated for the above-
472 mentioned scenarios, and the parameters were fixed based on the literature. This is a limitation of the present
473 study because the parameters adopted based on measurements made in other Mediterranean sites do not
474 necessarily apply to the Celone river basin. The choice of the scenarios was performed keeping in mind the
475 necessity of providing a wide range of realistic effects of wildfire and mitigation measures on soil loss and
476 runoff. Consequently, the above-mentioned parameters changed dramatically too. Thus, USLE_K was
477 assumed to vary from +80% for high-severity fire to no difference for the very low-severity fire. They were
478 the highest and lowest values reported in the literature, respectively. Similarly, CN2 was assumed to change
479 drastically (73 to 90 for Fr6 and Fr1, respectively).

480 According to the assumptions, wildfires have an important effect on the sedimentary response. The
481 increment related to the runoff was negligible in all the analysed scenarios. Lucas-Borja et al. (2019)
482 highlighted that the type of treatment (i.e. mulching or logging) did not influence the runoff generation in
483 their plots. Fr1 and Fr2 showed a dramatic increase in SSY for the three HRUs analysed, increasing in the

484 worst case (HRU 1, Sub. 55) from $1.26 \text{ t ha}^{-1} \text{ y}^{-1}$ (baseline) to $95.8 \text{ t ha}^{-1} \text{ y}^{-1}$ and to $59.9 \text{ t ha}^{-1} \text{ y}^{-1}$, respectively
485 (Figure 7). Malvar et al. (2017) and Wagenbrenner et al. (2015) evidenced that logging operations may
486 increase SSY mainly because of the trail generated by the passage of heavy machinery.

487 Fr5 and Fr6 showed a moderate increase of SSY that was quantified in 8.6 and $5 \text{ t ha}^{-1} \text{ y}^{-1}$ (HRU 1, Sub. 55),
488 respectively. These results agree with the Shakesby (2011) studies, which pointed out that from high to low-
489 severity fire, the effect on erosion may vary from more than two orders of magnitude or may not show
490 differences at all. From the modelling point of view, the difference in SSY between Fr5 and Fr6 was mainly
491 attributable to the USLE_K factor and, to a very small extent, to CN2 (-2 in Fr6) since all the other
492 parameters were unchanged. This result confirmed the USLE_K factor as a very sensitive parameter in soil
493 loss modelling. The difference in SSY between the Fr1 and Fr2 resulted from the integrated effect of several
494 parameters (USLE_C, CN2, and OV-N) that were differentiated in the two scenarios (Table III).

495 The post-fire mitigation measures have been widely implemented, but the assessment of their efficiency has
496 been limited to local studies mainly conducted at the hillslope scale (Girona-García et al., 2021). The authors
497 highlighted the need for studies on post-fire erosion mitigation measures, especially in high soil erosion
498 areas. In the present study, the mulching treatment (Fr3) reduced SSY ($20.2 \text{ t ha}^{-1} \text{ y}^{-1}$) compared with the
499 high-severity fire Fr2 producing a reduction of SSY (66%). This result confirmed the study by Fernandez et
500 al. (2011) carried out in Galicia, where the authors concluded that straw mulch application with 80% soil
501 cover reduced soil loss by 66%. Fr3 resulted in more effective mitigation than the moderate-severity fire and
502 erosion barriers. From the modelling point of view, this result is mainly attributable to the parameter
503 USLE_P, which was assumed equal to 0.343 for straw mulching (Fernandez et al., 2010). When moderate-
504 severity fire and erosion barriers were modelled (Fr4), SSY ranged from 19.8 to $26.2 \text{ t ha}^{-1} \text{ y}^{-1}$ in the three
505 analysed HRUs showing a reduction (56-61%) compared with Fr3. These results agree with the study by
506 Rulli et al. (2013), who determined a value of $24.1 \text{ t ha}^{-1} \text{ y}^{-1}$, and with Fernandez et al. (2011), who observed
507 a mean efficiency of barriers in retaining sediment of 58%.

508 **4.3 Future perspectives**

509 Despite the limits of the present study, the results clearly indicate that the rate of soil loss for the current land
510 use and management practices is much higher than the soil rate formation that was estimated for European

511 soils in $140 \text{ t km}^{-2} \text{ y}^{-1}$ (0.056 mm y^{-1}) by Verheijen et al. (2009). This study confirms that it is urgent to
512 reverse this trend by promoting soil loss mitigation measures (Montanarella and Panagos, 2021).
513 Ricci et al. (2020) analysed the efficiency and economic implications of some best management practices
514 (BMPs) like contour farming, no-tillage, and reforestation, for the public and private sectors. They concluded
515 that those BMPs, which the Apulia Region Rural Development Programme currently supports, effectively
516 reduce soil losses but have not yet been adopted at a large scale. Several barriers still exist that limit their
517 adoption (e.g., farmers' education, lack of awareness of soil erosion). Numerous actions are needed to favour
518 the adoption of BMPs, and important public economic resources are needed to support a plan for soil
519 protection.

520 In order to address these challenges, the EU's common agricultural policy may have an important role in
521 ensuring that agriculture is in line with the soil protection principles. The new European Green Deal (EGD)
522 with the "Farm to Fork" and the "zero pollution action plan" strategies will be central in preserving soil
523 systems and biodiversity (Montanarella and Panagos, 2021). Research and monitoring may play an important
524 role in reaching the EGD's goals.

525 In the next decades, increased fire risk is expected in the Mediterranean. Watershed management will need
526 fire prevention efforts and specific actions to protect and restore the river basins before disturbance occurs.
527 95% of fires are due to human activities (i.e. agricultural practices) or negligent behaviour and arson (Vilar
528 del Hoyo et al., 2009). It is, therefore, necessary to increase public perception and awareness of the risks of
529 wildfires and their impact on soil and water resources. Fire impact on soil is significant (Cerdà and
530 Robichaud, 2009), leading to an increase in soil erosion (Shakesby and Doerr, 2006). Hence, implementing
531 mitigation measures to reduce soil erosion is imperative and should be a part of every forest and soil
532 recovery strategy (Bento-Gonçalves et al., 2012). This study has shown the effectiveness of straw mulching,
533 seeding, and soil erosion barriers in reducing soil erosion. However, further studies and new monitoring
534 programs are needed to assess additional mitigation measures and adequately analyse their cost-
535 effectiveness.

536 **5. Conclusions**

537 This paper presents a study conducted in the Celone river basin, a Mediterranean watershed with an
538 intermittent river network. The SWAT model, calibrated with field measurements, was applied for the
539 current land use and land management practices for hydrology and sediment yield. The model adequately
540 reproduced the measured discharge for two monitoring periods: 1994-1996 and 2010-2011. It also
541 satisfactorily reproduced suspended sediment dynamics over the period 2010-2011, indicating that it may be
542 used to analyse the hydro-sedimentary response of the basin.

543 At the basin scale, results showed that the average soil loss estimated over a long period (1990-2011) is
544 much higher than the soil formation rate. These results reveal the need of promoting mitigation measures to
545 reduce soil losses.

546 Due to weather conditions and ignition sources, the basin is classified as a “high risk of fire” site. The
547 probability of wildfires and the risk of short and long-term post-fire contamination of surface water could
548 increase due to climate change in the near future. Watershed management may have an important role in
549 reducing the effects of wildfire on soil and water by implementing post-fire risk mitigation and restoration
550 measures.

551 The present work analyses six post-fire scenarios by modelling the basin’s response in terms of runoff and
552 SSY. It aims to provide a tool for post-fire risk management. The results showed that SWAT—a
553 hydrological and water quality model—may contribute to selecting the mitigation options to reduce soil
554 erosion after a fire. In addition, the model is also a useful tool for the post-fire risk assessment in terms of
555 water quality since it identifies the river segments where sediment-associated pollutants transported via
556 surface runoff could accumulate on the riverbed after fire events.

557 According to the assumption, high-severity fire vastly increases SSY at the basin and subbasin scales and
558 HRU levels. This study shows that a dramatic increase in soil erosion occurs in areas sensitive to erosion,
559 demonstrating that major efforts are needed to prevent forest fires and better manage the post-fire. The
560 results showed that a small part (2%) of the catchment is enough to cause a dramatic increase in soil loss
561 quantified at the basin scale by up to $12 \text{ t ha}^{-1} \text{ y}^{-1}$. Post-fire management is effective at mitigating fire impact
562 on soil erosion. In particular, post-fire mitigation measures such as emergency stabilisation (straw mulching
563 and seeding) and soil erosion barriers are better at reducing soil erosion than natural regeneration or logging

564 operations. This work also shows that further studies and field campaigns are needed to validate modelling
565 results for adequately analysing the cost-effectiveness of these measures.

566

567 **Credit Authors Statement**

568 All co-authors conceptualized the study. AMDG designed the model simulations and wrote the initial draft.
569 AMDG, RV, GFR, and TG collected input data. AMDG finalized the writing. All co-authors reviewed the
570 paper. AMDG wrote the revised manuscript. RV, OC, AMDG and ALP secure funding and were involved in
571 project administration.

572

573 **Declaration of competing interest**

574 The authors declare that they have no known competing financial interests or personal relationships that
575 could have appeared to influence the work reported in this paper.

576

577 **Acknowledgements**

578 This study was funded by the ERA4CS SERV_FORFIRE project. ERA4CS is an ERA-NET initiated by JPI
579 Climate, with co-funding by the European Union (Grant 690462).

580

581 **REFERENCES**

582 Abdelwahab O.M.M., Ricci G.F., De Girolamo A.M., Gentile F. 2018. Modelling soil erosion in a
583 Mediterranean watershed: Comparison between SWAT and AnnAGNPS models. Environmental
584 Research 166: 363-376. <https://doi.org/10.1016/j.envres.2018.06.029>.

585 Argentiero, I.; Ricci, G.F.; Elia, M.; D'Este, M.; Giannico, V.; Ronco, F.V.; Gentile, F.; Sanesi, G.

586 Combining Methods to Estimate Post-Fire Soil Erosion Using Remote Sensing Data. Forests 2021, 12, 1105.

587 <https://doi.org/10.3390/f12081105>

588 Arnold J.G., Srinivasan R., Muttiah R.S., Williams J.R. 1998. Large area hydrologic modeling and
589 assessment - Part 1: Model development. Journal of the American Water Resources Association,
590 34(1), 73-89. DOI: 10.1111/j.1752-1688.1998.tb05961.x.

591 Basso M., Vieira D.C.S., Ramos T.B., Mateus M. 2020. Assessing the adequacy of SWAT model to simulate
592 postfire effects on the watershed hydrological regime and water quality. *Land Degradation &*
593 *Development* 31 (5), 619-631

594 Bento-Gonçalves A., Vieira A., Úbeda X., Martín D. 2012. Fire and soils: Key concepts and recent advances
595 *Geoderma* 191, 3-13.

596 Bezak N., Mikoš M., Borrelli P., Alewell C., Alvarez P., Anache J.A.A., ..De Girolamo, A.M....Panagos P.
597 2021. Soil erosion modelling: A bibliometric analysis. *Environmental Research*, 111087.

598 Borrelli P., Alewell C., Alvarez P., Anache J.A.A., Baartman J., Ballabio C., ...De Girolamo A.M., Panagos
599 P. 2021. Soil erosion modelling: A global review and statistical analysis. *Science of the Total*
600 *Environment* 780 (146494)

601 Borrelli P., Panagos P., Langhammer J., Langhammer B., Schutt B. 2016. Assessment of the cover changes
602 and soil loss potential in European forestland: First approach to derive indicators to capture the
603 ecological impacts on soil-related forest ecosystems. *Ecological Indicators* 60: 1208–1220.
604 <https://doi.org/10.1016/j.ecolind.2015.08.053>

605 Bowman D.M.J.S. et al. Fire in the Earth system. *Science* (New York, N.Y.) 324, 481–485 (2009).

606 Brouziyne Y., De Girolamo A.M., Aboubdillah A., Benaabidate L., Bouchaou L., Chehbouni A. 2021.
607 Modeling alterations in flow regimes under changing climate in a Mediterranean watershed: An
608 analysis of ecologically-relevant hydrological indicators. *Ecological Informatics*, 61, 101219.
609 <https://doi.org/10.1016/j.ecoinf.2021.101219>.

610 Camia A., Amatulli, G. Weather Factors and Fire Danger in the Mediterranean. In Chuvieco, E. (ed.) *Earth*
611 *Observation of Wildland Fires in Mediterranean Ecosystems*, 71–82 (Springer-Verlag, Berlin, 2009).

612 Campos I.M.A.N., Abrantes N., Vidal T., Bastos A.C., Gonçalves F., Keizer J.J. 2012. Assessment of the
613 toxicity of ash-loaded runoff from a recently burnt eucalypt plantation. *European Journal of Forest*
614 *Research*, 131(6), 1889–1903. [Doi: 10.1007/s10342-012-0640-7](https://doi.org/10.1007/s10342-012-0640-7)

615 Cakir R., Gerino M., Volk M., Sánchez-Pérez J.M. 2020. Assessment of ecological function indicators
616 related to nitrate under multiple human stressors in a large watershed. *Ecological Indicators* 111,
617 106016

618 Cerdà A., 1998. Changes in overland flow and infiltration after a rangeland fire in a Mediterranean
619 scrubland. *Hydrological Processes*, 12, 1031-1042.

620 Cerdà A., Doerr S.H. 2008. The effect of ash and needle cover on surface runoff and erosion in the
621 immediate post-fire period. *Catena* 73(3), 256-263.

622 Cerdà A., Robichaud P., 2009. Fire effects on soil infiltration. In: Cerdà, A., Robichaud, P. (Eds.), *Fire
623 Effects on Soils and Restoration Strategies*. Science Publishers, Enfield, New Hampshire, pp. 81-
624 103.

625 Cerdan O., Govers G., Le Bissonnais Y., et al. 2010. Rates and spatial variations of soil erosion in Europe: a
626 study based on erosion plot data. *Geomorphology*, 122 (1–2) (2010), pp. 167-177

627 Civil Protection Agency, 2018. Regional Plan 2018-2020. [https://protezionecivile.puglia.it/pubblicazioni-
628 incendi/piano-regionale-aib-2018-2020/](https://protezionecivile.puglia.it/pubblicazioni-incendi/piano-regionale-aib-2018-2020/) Last access 23th November 2020.

629 Chessman B.C., 1986. Impact of the 1983 wildfires on river water quality in East Gippsland, Victoria.
630 *Australian Journal of Marine and Freshwater Research* 37 (3), 399–420.

631 Coschignano G., Nicolai A., Ferrari E., Cruscomagno F., Iovino F. 2019. Evaluation of hydrological and
632 erosive effects at the basin scale in relation to the severity of forest fires. *iForest* 12:427-434.
633 Doi:10.3832/ifor2878-012

634 D'Ambrosio E., Gentile F., De Girolamo A.M. 2020a. Assessing the sustainability in water use at the basin
635 scale through water footprint indicators. *Journal of Cleaner Production*, 244. 118847.
636 <https://doi.org/10.1016/j.jclepro.2019.118847>

637 D'Ambrosio E., Ricci G.F., Gentile F., De Girolamo A.M. 2020b. Using water footprint concepts for water
638 security assessment of a basin under anthropogenic pressures. *Science of The Total Environment*
639 748, 141356. 10.1016/j.scitotenv.2020.141356

640 De Girolamo A.M., Di Pillo R., Lo Porto A., Todisco M.T., Barca E. 2018. Identifying a reliable method for
641 estimating suspended sediment load in a temporary river system. *Catena* 165: 442-453. Doi:
642 [10.1016/j.catena.2018.02.015](https://doi.org/10.1016/j.catena.2018.02.015)

643 De Girolamo A., Barca E., Pappagallo E., Lo Porto A. 2017a. Simulating ecologically relevant hydrological
644 indicators in a temporary river system. *Agricultural Water Management* 180(Part B): 194-204, doi:
645 10.1016/j.agwat.2016.05.034

646 De Girolamo A., Bouroui F., Buffagni A., Pappagallo G., Lo Porto A. 2017b. Hydrology under climate
647 change in a temporary river system: Potential impact on water balance and flow regime. *River*
648 *Research and Applications* 33:1219–1232. doi: DOI10.1002/rra.3165

649 De Girolamo A.M., Pappagallo G., Lo Porto A. 2015. Temporal variability of suspended sediment transport
650 and rating curves in a Mediterranean river basin: The Celone (SE Italy). *Catena* 128: 135-143.
651 DOI:10.1016/j.catena.2014.09.020

652 De Girolamo A.M., Lo Porto A, 2020. Source Apportionment of Nutrient Loads to a Mediterranean River
653 and Potential Mitigation Measures. *Water* 12 (2), 577. <https://doi.org/10.3390/w12020577>.

654 Doerr S.H., Shakesby R.A., MacDonald L.H. 2009. Soil water repellency: a key factor in post-fire erosion.
655 In: *Fire effects on soil and restoration strategies*. Ed. Cerdà A. & Robichaud P.R. Taylor & Francis
656 Group NW

657 Di Piazza G.V., Di Stefano C., Ferro V. 2007. Modelling the effects of a bushfire on erosion in a
658 Mediterranean basin, *Hydrological Sciences Journal* 52:6, 1253-1270, DOI: 10.1623/hysj.52.6.1253

659 Esteves T.C.J. Kirkby M.J., Shakesby R.A., Ferreira A.J.D., Soares J.A.A., Irvine B.J., Ferreira C.S.S.,
660 Coelho C.O.A., Bento C.P.M., Carreiras M.A. 2012. Mitigating land degradation caused by wildfire:
661 application of PESERA model to fire-affected sites in central Portugal. *Geoderma*, 191, 40-50.

662 Fortesa J., Ricci G.F., García-Comendador J., Gentile F., Estrany J., Sauquet E., Datry T., De Girolamo A.M.
663 2021. Analysing hydrological and sediment transport regime in two Mediterranean intermittent
664 rivers. *Catena*, 196, DOI: 10.1016/j.catena.2020.104865

665 European Commission 2019. CLIM 035 (03 Dec 2019). [https://www.eea.europa.eu/data-and-](https://www.eea.europa.eu/data-and-maps/indicators/forest-fire-danger-3/assessment)
666 [maps/indicators/forest-fire-danger-3/assessment](https://www.eea.europa.eu/data-and-maps/indicators/forest-fire-danger-3/assessment)

667 Efthimiou N., Psomiadis E., Panagos P. 2020. Fire severity and soil erosion susceptibility mapping using
668 multi-temporal Earth Observation data: The case of Mati fatal wildfire in Eastern Attica, Greece.
669 *Catena* 187, 104320.

670 Fernández C., Vega J.A., Vieira D.C.S. 2010. Assessing soil erosion after fire and rehabilitation treatments
671 in NW Spain: Performance of RUSLE and revised Morgan–Morgan–Finney models. *Land*
672 *Degradation & Development* 21 (1), 58–67

673 Fernández C., Vega J.A. Jiménez E., Fonturbel M.T. 2011. Effectiveness of three post-fire treatments at
674 reducing soil erosion in Galicia (NW Spain), *Int. J. Wildland Fire*, 20, 104–114.
675 tion & Development, 21 (1), 58–67.

676 Fernández C., Vega J.A. 2016. Evaluation of RUSLE and PESERA models for predicting soil erosion losses
677 in the first year after wildfire in NW Spain. *Geoderma*, 273, 64–72.
678 <https://doi.org/10.1016/j.geoderma.2016.03.016>

679 Fernández C., Vega J.A. 2018. Evaluation of the rusle and disturbed wepp erosion models for predicting soil
680 loss in the first year after wildfire in NW Spain. *Environmental Research* 165. Doi:
681 [10.1016/j.envres.2018.04.008](https://doi.org/10.1016/j.envres.2018.04.008)

682 Fernandéz-Anez N., Krasovskiy A., ...et al. 2021. Current wildland fire patterns and challenges in Europe:
683 synthesis of national perspectives. *Air, Soil and Water Research* 14, 1-19. Doi:
684 [10.1177/11786221211028185](https://doi.org/10.1177/11786221211028185).

685 Foucher A., Evrard O., Cerdan O., Chabert C., Lefèvre I., Vandromme R., Salvador-Blanes S. 2021.
686 Deciphering human and climatic controls on soil erosion in intensively cultivated landscapes after
687 1950 (Loire Valley, France). *Anthropocene* 34, 100287, Doi: [10.1016/j.ancene.2021.100287](https://doi.org/10.1016/j.ancene.2021.100287)

688 Gamvroudis C., Nikolaidis N.P., Tzoraki O., Papadoulakis V., Karalemas N. 2015. Water and sediment
689 transport modeling of a large temporary river basin in Greece. *Science of the Total Environment*
690 508, 354-365.

691 Ganteaume A. et al. 2013. A review of the main driving factors of forest fire ignition over Europe.
692 *Environmental management* 51, 651–62.

693 García-Comendador J., Fortesa J., Calsamiglia A., Calvo-Cases A., Estrany J. 2017. Post-fire hydrological
694 response and suspended sediment transport of a terraced Mediterranean catchment. *Earth Surface*
695 *Processes and Landforms* 42 (14), 2254–2265

696 Girona-García A., Vieira D.C.S., Silva J., Fernández C., Robichaud P.R., Keizer J.J. 2021. Effectiveness of
697 post-fire soil erosion mitigation treatments: A systematic review and meta-analysis, *EarthScience*
698 *Reviews*, 217, 103611. <https://doi.org/10.1016/j.earscirev.2021.103611>

699 Grangeon T., Vandromme R., Cerdan O., De Girolamo A.M., Lo Porto A. 2021. Modelling forest fire and
700 firebreak scenarios in a mediterranean mountainous catchment: Impacts on sediment loads. Journal
701 of Environmental Management 289 (112497). Doi: 10.1016/j.jenvman.2021.112497

702 Havel A., Tasdighi A., Arabi M. 2018. Assessing the hydrologic response to wildfires in mountainous
703 regions. Hydrology and Earth System Sciences, 22(4), 2527–2550.

704 Ice G.G., Neary D.G., Adams P.W. 2004. Effects of wildfire on soils and watershed processes. Journal of
705 Forestry 102(6):16-20.

706 Kampf, S.K., Gannon, B.M., Wilson, C., Saavedra, F., Miller, M.E., Heldmyer, A., Livneh, B., Nelson, P.,
707 MacDonald, L., 2020. PEMIP: Post-fire erosion model inter-comparison project. Journal of
708 Environmental Management, 268, 110704.

709 Karamesouti M., Petropoulos G., Papanikolaou I., Kairis O., Kosmas K. 2016. Erosion rate predictions from
710 PESERA and RUSLE at a Mediterranean site before and after a wildfire: comparison & implications.
711 Geoderma 261: 44–58. <https://doi.org/10.1016/j.geoderma.2015.06.025>

712 Kirkby M.J., Jones R.J.A., Irvine B., Gobin A, Govers G., Cerdan O., Van Rompaey A.J.J., Le Bissonnais
713 Y., Daroussin J., King D., Montanarella L., Grimm M., Vieillefont V., Puigdefabregas J., Boer M.,
714 Kosmas C., Yassoglou N., Tsara M., Mantel S., Van Lynden G.J., Huting J. 2004. European Soil
715 Bureau Research Report No.16, EUR 21176, 18pp. and 1 map in ISO B1 format. Office for Official
716 Publications of the European Communities, Luxembourg

717 Kirkby M., Irvine B., Jones R., Govers G., PESERA team. 2008. The PESERA coarse scale erosion model
718 for Europe I. Model rationale and implementation. European Journal of Soil Science 59(6):1293–
719 1306. <https://doi.org/10.1111/j.1365-2389.2008.01072.x>

720 Lasaponara R., Aromando A., Cardettini G., Proto M. 2018. Fire Risk Estimation at Different Scales of
721 Observations: An Overview of Satellite Based Methods Computational Science and Its Applications
722 – ICCSA 2018

723 Lanorte A., Cillis G., Calamita G., Nolè G., Pilogallo A., Tucci B., De Santis F. 2019. Integrated approach of
724 RUSLE, GIS and ESA Sentinel-2 satellite data for post-fire soil erosion assessment in Basilicata
725 region (Southern Italy), Geomatics, Natural Hazards and Risk, 10:1, 1563-1595, DOI:
726 10.1080/19475705.2019.1578271

727 Larsen I.J., MacDonald L.H. 2007. Predicting postfire sediment yields at the hillslope scale: Testing RUSLE
728 and disturbed WEPP. *Water Resources Research*, 43, W11412. Doi:10.1029/2006WR005560

729 Lopes A.R., Girona-García A., Corticeiro S., Martins R., Keizer J., Vieira D.C.S., 2021. What is wrong with
730 post-fire soil erosion modelling? A meta-analysis on current approaches, research gaps, and future
731 directions. *Earth Surf. Process. Landf.* In press. DOI: 10.1002/esp.5020

732 Lucas-Borja M.E., Calsamiglia A., Fortesa J., García-Comendador J., Lozano Guardiola E., García-Orenes
733 F., Gago J., Estrany J. 2018. The role of wildfire on soil quality in abandoned terraces of three
734 Mediterranean micro-catchments. *Catena* 170. 246-256.

735 Lucas-Borja, M.E.; González-Romero, J.; Plaza-Álvarez, P.A.; Sagra, J.; Gómez, M.E.; Moya, D.; Cerdà, A.;
736 de las Heras, J. The impact of straw mulching and salvage logging on post-fire runoff and soil
737 erosion generation under Mediterranean climate conditions. *Sci. Total Environ.* 2019, 654, 441–451,
738 doi:10.1016/J.SCITOTENV.2018.11.161

739 Lucas-Borja M.E. 2021. Efficiency of post-fire hillslope management strategies: gaps of knowledge *Current*
740 *Opinion in Environmental Science & Health* <https://doi.org/10.1016/j.coesh.2021.100247>

741 Malvar, M.C.; Silva, F.C.; Prats, S.A.; Vieira, D.C.S.; Coelho, C.O.A.; Keizer, J.J. Short-term effects of
742 post-fire salvage logging on runoff and soil erosion. *For. Ecol. Manage.* 2017, 400, 555–567,
743 doi:10.1016/J.FORECO.2017.06.031

744 Mayor, A.G., Bautista, S., Llovet, J., Bellot, J. 2007. Post-fire hydrological and erosional responses of a
745 Mediterranean landscape: Seven years of catchment-scale dynamics. *Catena*, 71, 68-75.

746 Mataix-Solera J., Cerdà A., Arcenegui V., Jordán A., Zavala L.M. 2011. Fire effects on soil aggregation: A
747 review. *Earth-Science Reviews* 109 (1–2), 44-60. 10.1016/j.earscirev.2011.08.002

748 Montanarella L., Panagos P. 2021. The relevance of sustainable soil management within the European Green
749 Deal. *Land Use policy* 100, 104950. Doi: 10.1016/j.landusepol.2020.104950.

750 Moriasi D.N., Arnold J.G., Van Liew M.W., Bingner R.L., Harmel R.D., Veith T.L. 2007. Model evaluation
751 guidelines for systematic quantification of accuracy in watershed simulations. *Trans. ASABE* 50,
752 885–900.

753 Miller J.D., Nyhan J.W., Yool S.R. 2003. Modeling potential erosion due to the Cerro Grande fire with a
754 GIS-based implementation of the Revised Universal Soil Loss Equation, *Int. J. Wildland Fire*, 12,
755 85– 100.

756 Myronidis D.I., Emmanouloudis D.A., Mitsopoulos I.A., Riggos E.E. 2010. Soil Erosion Potential after Fire
757 and Rehabilitation Treatments in Greece, in: *Environ. Model Assess.*, 15, 239–250,
758 doi:10.1007/s10666-009-9199-1

759 Neary D.G., Klopatek C.C., DeBano L.F., Ffolliott P.F. 1999. Fire effects on belowground sustainability: a
760 review and synthesis. *Forest Ecology and Management* 122, 51–71.

761 Neary D.G., Ryan K.C., DeBano L.F. (Eds.) 2005. (revised 2008). *Wildland fire in ecosystems: effects of*
762 *fire on soils and water. Gen. Tech. Rep. RMRS-GTR-42-vol.4.* Ogden, UT: U.S. Department of
763 Agriculture, Forest Service, Rocky Mountain Research Station, 250 pp.

764 Neitsch S.L., Arnold J.G., Kiniry J.R., Williams J.R. 2011. *Soil and Water Assessment Tool Theoretical*
765 *Documentation. Version, 2000, USDA Agricultural Research Service and Texas Agricultural*
766 *Experiment Station, Temple, TX.*

767 Nunes B., Silva V., Campos I., Pereira J. L., Pereira P., Keizer J. J., ...Abrantes N. 2017. Off-site impacts of
768 wildfires on aquatic systems—Biomarker responses of the mosquitofish *Gambusia holbrooki*.
769 *Science of the Total Environment*, 581, 305–313. <https://doi.org/10.1016/j.scitotenv.2016.12.129>

770 Nunes J.P., Quintanilla P.N., Santos J.M., Serpa D., Carvalho-Santos C., Rocha J., Keizer J.J., Keestra S.D.,
771 2018. Afforestation, subsequent forest fires and provision of hydrological services: a model-based
772 analysis for a Mediterranean mountainous catchment. *Land Degradation & Development*, 29, 776-
773 788.

774 Olivella M.A., Ribalta T.G., de Febrer A.R., Mollet J.M., de las Heras F.X.C. 2006. Distribution of
775 polycyclic aromatic hydrocarbons in riverine waters after Mediterranean forest fires. *Science of the*
776 *Total Environment* 355, 156–166.

777 Panagos P., Borrelli P., Meusburger K., van der Zanden E.H., Poesen J., Alewell K. 2015a. Modelling the
778 effect of support practices (P-factor) on the reduction of soil erosion by water at European scale
779 *Environmental Science & Policy* Volume 51, August 2015, Pages 23-34

780 Panagos, P., Borrelli, P., Meusburger, C., Alewell, C., Lugato, E., Montanarella, L., 2015b. Estimating the
781 soil erosion cover-management factor at European scale. *Land Use policy journal*. 48C, 38-50. ,
782 doi:10.1016/j.landusepol.2015.05.021

783 Panagos P., Borrelli P., Poesen J., Ballabio C., Lugato E., Meusburger K., Montanarella L., Alewell C.,
784 2015c. The new assessment of soil loss by water erosion in Europe. *Environmental Science &*
785 *Policy*, 54, 438-447. Doi: 10.1016/j.envsci.2015.08.012

786 Panagos P., Imeson A., Meusburger K., Borrelli P., Poesen J, Alewell C. 2016. Soil Conservation in Europe:
787 Wish or Reality? *Land Degrad. Develop.* 27: 1547-1551. <https://doi.org/10.1002/ldr.2538>Citations:
788 77

789 Pausas, J.G., Llovet, J., Rodrigo, A., Vallejo, R., 2008. Are wildfires a disaster in the Mediterranean basin? –
790 A review. *International Journal of Wildland Fires*, 17(6), 713-723.

791 Pulighe G., Bonati G., Colangeli M., Traverso L., Lupia F., Altobelli F., Dalla Marta A., Napoli M. 2019.
792 Predicting streamflow and nutrient loadings in a semiarid Mediterranean watershed with ephemeral
793 streams using the SWAT model. *Agronomy*, 10, 2, doi:10.3390/agronomy10010002.

794 Poesen J., 2018. Soil erosion in the Anthropocene: research needs. *Earth Surf. Process. Landforms* 84, 64–
795 84. <https://doi.org/10.1002/esp.4250>

796 Ricci G, De Girolamo AM, Abdelwahab O, Gentile F. 2018. Identifying sediment source areas in a
797 mediterranean watershed using the swat model. *Land Degradation & Development* 29: 1233-1248.
798 doi: 10.1002/ldr.2889.

799 Ricci G.F., Jeong J., De Girolamo A.M., Gentile F., 2020. Effectiveness and feasibility of different
800 management practices to reduce soil erosion in an agricultural watershed. *Land Use Policy*, 90
801 (104306). <https://doi.org/10.1016/j.landusepol.2019.104306>.

802 Ruffault J., Moron V., Trigo R., Curt T. 2016. Daily synoptic conditions associated with large fire
803 occurrence in mediterranean france: evidence for a wind-driven fire regime. *International Journal of*
804 *Climatology*.

805 Rulli M.C. Rosso R. 2005. Modeling catchment erosion after wild-fires in the San Gabriel Mountains of
806 southern California, *Geo-phys. Res. Lett.*, 32/19, 1–4, doi:10.1029/2005GL023635

807 Rulli M.C. Rosso R. 2007. Hydrologic response of upland catchments to wildfires, *Adv. Water Resour.*, 30,
808 2072–2086

809 Rulli M.C., Offeddu L., Santini M. 2013. Modeling post-fire water erosion mitigation strategies. *Hydrol.*
810 *Earth Syst. Sci.*, 17, 2323–2337. <https://doi.org/10.5194/hess-17-2323-2013>

811 Sebastian-Lopez A., Salvador-Civil R., Gonzalo-Jimenez, J., San-Miguel-Ayanz, J., 2008. Integration of
812 socio-economic and environmental variables for modeling long-term fire danger in southern Europe.
813 *European Journal of Forest Research* 127 (2), 149–163

814 San-Miguel-Ayanz J. et al. Comprehensive Monitoring of Wildfires in Europe: The European Forest Fire
815 Information System (EFFIS). In Tiefenbacher, J. (ed.) *Approaches to Managing Disaster - Assessing*
816 *Hazards, Emergencies and Disaster Impacts*, chap. 5, <http://dx.doi.org/10.5772/28441> (InTech,
817 2012).

818 Shakesby R.A., Doerr S.H. 2006. Wildfire as a hydrological and geo-morphological agent. *Earth-Science*
819 *Reviews*, 74(3–4), 269–307.

820 Shakesby R.A. 2011. Post-wildfire soil erosion in the Mediterranean: review and future research directions.
821 *Earth-Science Reviews* 105, 71–100.

822 Smith H.G., Sheridan G J., Lane P.N.J., Nyman P., Haydon S. 2011. Wildfire effects on water quality in
823 forest catchments: A review with implications for water supply. *Journal of Hydrology* 396 (2011)
824 170–192.

825 Stoof C.R. Ferreira A.J.D., Mol W., Van den Berg J., De Kort A., Drooger S., Slingerland E.C., Mansholt
826 A.U., Ferreira C.S.S., Ritsema C.J. 2015. Soil surface changes increase runoff and erosion risk after
827 a low–moderate severity fire. *Catena* 239-240. 58-67

828 Tecle A., Neary D. 2015. Water Quality Impacts of Forest Fires. *J Pollut Eff Cont* 3, 140. doi:10.4172/2375-
829 4397.1000140

830 Turco M., von Hardenberg J., AghaKouchak A., Llasat M.C., Provenzale A., Trigo R.M. 2017. On the key
831 role of droughts in the dynamics of summer fires in Mediterranean Europe *Scientific Reports* 7: 81
832 DOI:10.1038/s41598-017-00116-9

833 Urbieto I. R. et al. Fire activity as a function of fire-weather seasonal severity and antecedent climate across
834 spatial scales in southern europe and pacific western usa. *Environmental Research Letters* 10,
835 114013 (2015).

836 Verkaik I., Rieradevall M., Cooper S.D., Melack J.M., Dudley T.L., Prat N. 2013. Fire as a disturbance in
837 Mediterranean climate streams. *Hydrobiologia* 719: 353–382. [https://doi.org/10.1007/s10750-013-](https://doi.org/10.1007/s10750-013-1463-3)
838 1463-3

839 Vieira D.C.S., Fernández C., Vega J.A., Keizer J.J. 2015. Does burn severity affect the post-fire runoff and
840 interrill erosion response? A review based on meta-analysis of field rainfall simulation data *J.*
841 *Hydrol.*, 523 (2015), pp. 452-464, 10.1016/j.jhydrol.2015.01.071

842 Vieira D.C.S., Malvar M.C., Martins M.A.S., Serpa D., Keizer J.J. 2018. Key factors controlling the post-fire
843 hydrological and erosive response at micro-plot scale in a recently burned Mediterranean forest.
844 *Geomorphology*, 319, 161–173. <https://doi.org/10.1016/j.geomorph.2018.07.014>

845 Vigiak O., Malagó, A., Bouraoui F. Vanmaercke M., Obreja F., Poesen J., Habersack H., Fehér J., Grošelj S.
846 2017. Modelling sediment fluxes in the Danube River Basin with SWAT. *Science of The Total*
847 *Environment* 599–600, 992-1012

848 Wagenbrenner, J.W.; MacDonald, L.H.; Coats, R.N.; Robichaud, P.R.; Brown, R.E. Effects of post-fire
849 salvage logging and a skid trail treatment on ground cover, soils, and sediment production in the
850 interior western United States. *For. Ecol. Manage.* 2015, 335, 176–193,
851 doi:10.1016/J.FORECO.2014.09.016.

852 Waidler D., White M., Steglich E., Wang S., Williams J., Jones C.A., Srinivasan R. 2009. Conservation
853 Practice Modeling guide for SWAT and APEX Modeling-Guide
854 <https://swat.tamu.edu/media/57882/Conservation-Practice-Modeling-Guide.pdf>

855 Wischmeier W.H., Smith D.D. 1978. Predicting rainfall lossess: A guide to conservation planning. USDA
856 Agricultural Handbook No. 537. U.S. Gov. Print. Office, Washinton D.C.

857 Williams J.R., Berndt H.D. 1977. Sediment yield prediction based on watershed hydrology. 20(6):
858 <https://doi.org/10.13031/2013.35710>

859 Zema D.A. 2021. Postfire management impacts on soil hydrology. *Current Opinion in Environmental*
860 *Science & Health* 2021, 21:100252

861 Zema D.A., Nunes J.P., Lucas-Borja M.E. 2020. Improvement of seasonal runoff and soil loss predictions by
862 the MMF (Morgan-Morgan-Finney) model after wildfire and soil treatment in Mediterranean forest
863 ecosystems. *Catena*, 188, 104415. [10.1016/j.catena.2019.104415](https://doi.org/10.1016/j.catena.2019.104415)

864